

# Activation of the Redox-Regulated Molecular Chaperone Hsp33—A Two-Step Mechanism

Johannes Graumann,<sup>1</sup> Hauke Lilie,<sup>4</sup> Xianli Tang,<sup>1</sup>  
Katherine A. Tucker,<sup>1</sup> Jörg H. Hoffmann,<sup>1</sup>  
J. Vijayalakshmi,<sup>2</sup> Mark Saper,<sup>2,3</sup>  
James C.A. Bardwell,<sup>1</sup> and Ursula Jakob<sup>1,5</sup>

<sup>1</sup>Department of Biology

<sup>2</sup>Biophysics Research Division

<sup>3</sup>Department of Biological Chemistry  
University of Michigan

Ann Arbor, Michigan 48109

<sup>4</sup>Department of Biotechnology

University of Halle

Halle, Germany

## Summary

**Background:** Hsp33 is a novel redox-regulated molecular chaperone. Hsp33 is present in the reducing environment of the cytosol and is, under normal conditions, inactive. The four highly conserved cysteines found in Hsp33 constitute a novel zinc binding motif. Upon exposure to oxidative stress, Hsp33's chaperone activity is turned on. This activation process is initiated by the formation of two intramolecular disulfide bonds. Recently, the 2.2 Å crystal structure of Hsp33 has been solved, revealing that Hsp33 is present as a dimer in the structure (Vijayalakshmi et al., this issue, 367–375 [1]).

**Results:** We show here that oxidized, highly active Hsp33 is a dimer in solution. In contrast, reduced and inactive Hsp33 is monomeric. The incubation of reduced Hsp33 in H<sub>2</sub>O<sub>2</sub> leads to the simultaneous formation of two intramolecular disulfide bonds and the concomitant release of zinc. This concentration-independent step is followed by a concentration-dependent association reaction. The dimerization of Hsp33 requires highly temperature-sensitive structural rearrangements. This allows Hsp33's activation process to be greatly accelerated at heat shock temperatures.

**Conclusions:** The regulation of Hsp33's chaperone function is highly sophisticated. On a transcriptional level, Hsp33 is under heat shock control. This increases the concentration of Hsp33 under heat and oxidative stress, a process that favors dimerization, a critical step in Hsp33's activation reaction. On a posttranslational level, Hsp33 is redox regulated. Dimerization of disulfide-bonded Hsp33 monomers leads to the formation of two extended, putative substrate binding sites. These sites might explain Hsp33's high and promiscuous affinity for unstructured protein folding intermediates.

## Introduction

Hsp33 is a novel molecular chaperone with a unique mode of functional regulation. Hsp33's chaperone activ-

ity is regulated by the redox conditions of the environment [2–4]. Under reducing conditions, Hsp33 is inactive. All four conserved cysteines in Hsp33 are in the reduced, thiolate anion state, coordinate one zinc atom, and constitute a novel zinc binding motif [5]. Upon exposure to oxidizing conditions such as H<sub>2</sub>O<sub>2</sub>, two intramolecular disulfide bonds form in Hsp33 [2, 6]. These disulfide bonds connect the two neighboring cysteines Cys232–Cys234 and Cys265–Cys268 [6]. The oxidation of Hsp33's disulfide bonds is accompanied by the release of zinc and leads to the activation of Hsp33's chaperone function. In its oxidized and activated state, Hsp33 is able to recognize and bind aggregation-sensitive folding intermediates and can prevent nonspecific side reactions such as aggregation. In vivo thiol-trapping experiments of Hsp33's cysteines as well as genetic studies using Hsp33 deletion mutants suggest that the redox regulation of Hsp33's chaperone function plays an important role in protecting cells against the deleterious effects of reactive oxygen species [2]. Under nonstress conditions, the cytoplasmic Hsp33 is predominantly in its reduced, inactive state. Oxidizing conditions lead to the accumulation of disulfide-bonded, activated Hsp33 in the cytoplasm of *Escherichia coli*. Deletion mutants in Hsp33 show an increased sensitivity toward oxidative stress treatment [2].

Over the past few years, an increasing number of redox-regulated proteins have been identified. These proteins include the prokaryotic oxidative stress transcription factor OxyR [7]; the antisigma factor RsrA [8]; the oxidative stress transcription factor of yeast, Yap1 [9–11]; several zinc finger transcription factors; and protein kinase C [12]. A common feature among all of these proteins, including Hsp33, is the oxidation-induced formation of disulfide bonds. Highly reactive cysteines in these redox-regulated proteins sense changes in the redox environment and quickly translate them into changes in protein conformation and activity. However, these proteins differ in their individual mechanisms and the functional consequences of disulfide bond formation. Disulfide bond formation activates OxyR and induces conformational changes that allow tetrameric OxyR to initiate antioxidant gene transcription in *E. coli* [7]. In contrast, disulfide bond formation inactivates the antisigma factor RsrA [8]. This also leads to the initiation of antioxidant gene transcription, since disulfide-bonded and inactivated RsrA is no longer capable of interacting with and inhibiting the transcription factor sigma R. Sigma R, in its unbound form, now initiates the transcription of antioxidant genes such as thioredoxin reductase (*trxB*) in *Streptomyces coelicolor*.

Oxidation-induced disulfide bond formation leads to the activation of Hsp33's chaperone function in vitro and presumably also in vivo [2]. The recently solved crystal structure of Hsp33 revealed that Hsp33 forms a dimer in the crystal structure [1]. The finding that the

<sup>5</sup>Correspondence: ujakob@umich.edu

most conserved residues in Hsp33 are involved in the dimer formation suggests that dimerization is very important for Hsp33 function. We hypothesized that a change in Hsp33's oligomerization state might be part of its redox regulation. We report here that the mechanism of Hsp33's activation involves dimerization and follows an apparent unimolecular reaction. The first step is the simultaneous formation of both disulfide bonds in Hsp33, a process that is paralleled by the concomitant release of zinc from the zinc binding domain. Subsequently, dimerization of the oxidized Hsp33 monomers takes place and leads to the accumulation of highly active Hsp33 species. This activation by oxidative dimerization sheds new light on Hsp33's unique mode of functional regulation.

## Results and Discussion

### Construction of Inactive and Fully Active Hsp33 Mutants

To analyze the activation mechanism of a protein, it is absolutely essential to define the starting and the end point of the activation. The extent of the interaction between a chaperone and its substrate protein depends on both the activity of the chaperone and the folding state of the substrate [13]. It is, therefore, desirable to first calibrate the chaperone activity assay with inactive and fully active chaperone protein and to determine the chaperone concentration range over which this assay is linear.

To assess the reactivation kinetics of reduced, inactive Hsp33 upon incubation in the physiological oxidant  $H_2O_2$ , Hsp33's influence on the aggregation process of refolding luciferase was monitored. This chaperone assay has previously been used to study the role of zinc in the reactivation reaction of Hsp33 [5].

To generate a completely inactive mutant of Hsp33, we decided to test a cysteine-free mutant of Hsp33 in which all of the cysteines were replaced by aspartic acid or serine. Since it has been shown that disulfide bond formation is a prerequisite for the successful activation of Hsp33 [2], a cysteine-free mutant was predicted to be inactive. To construct the cysteine-free Hsp33 mutant, five of the six cysteines were substituted with serine. The remaining cysteine, C141, was substituted with aspartic acid because almost 50% of all known Hsp33 homologs harbor aspartic acid at that position in the protein. It was, therefore, reasoned that a cysteine to aspartic acid substitution at this position is less likely to disrupt the function of Hsp33 than is a serine substitution. The cysteine-free mutant protein was overexpressed in a BL21 variant that contained a null mutation in the gene for *hsp33* and was purified to homogeneity. Apart from a slightly increased sensitivity toward proteolysis, the cysteine-free Hsp33 mutant behaved very much like the reduced Hsp33 wild-type protein. Both are inactive in our chaperone activity assay (Figure 1). Not even a 5-fold molar excess of the cysteine-free Hsp33 mutant showed an influence on the aggregation behavior of luciferase. This result confirmed the findings in our studies of reduced, metal-free Hsp33, which also showed no chaperone activity [5], and clearly excluded

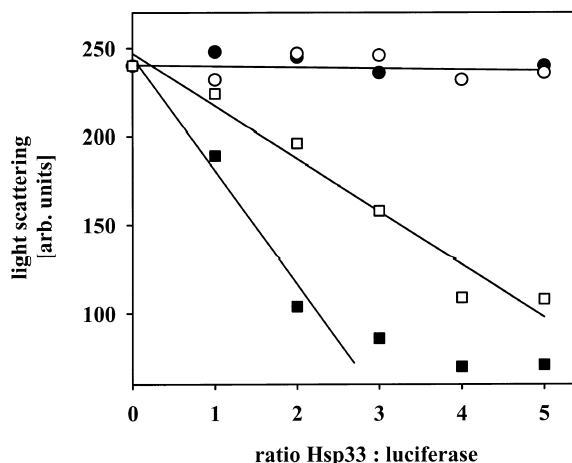


Figure 1. Influence of Hsp33 on the Aggregation Process of Chemically Denatured Luciferase

The light scattering signal of luciferase (48 nM) was recorded 6 min after the start of the renaturation process in the absence of additional protein or in the presence of increasing amounts of inactive, cysteine-free mutant (solid circle); active Hsp33DCCSSS mutant (solid square); inactive, reduced wild-type Hsp33 (open circle); and reoxidized wild-type Hsp33 (open square).

the possibility that zinc release of Hsp33 alone is sufficient for the activation process of Hsp33. The formation of the correct disulfide bond(s) in Hsp33 is absolutely required for the activation process of the chaperone.

To dissect the reasons for the inactivity of the cysteine-free Hsp33, various combinations of mutations within the conserved cysteines were constructed, and the proteins were overexpressed, purified, and tested. One mutant protein, Hsp33DCCSSS, in which the two nonconserved cysteines, Cys141D and Cys239S, and two of the conserved cysteines, Cys265S and Cys268S, were replaced with either aspartic acid or serine (see Experimental Procedures for our mutant nomenclature), was completely oxidized and was present in a highly active conformation when purified (Figure 1). This was in sharp contrast to wild-type Hsp33, which is predominantly reduced and inactive after purification. A 3-fold molar excess of this fully active Hsp33 mutant was capable of completely preventing the aggregation of refolding luciferase. The suppression of the aggregation of luciferase in the presence of a 5-fold molar excess of this fully active DCCSSS mutant Hsp33 was used in all subsequent studies as a measure of 100% chaperone activity. The influence of a 5-fold molar excess of the inactive, cysteine-free Hsp33 mutant was taken as 0% chaperone activity.

To establish the linear range of our chaperone assay, increasing concentrations of reoxidized, activated wild-type Hsp33 were tested for their influence on the aggregation behavior of luciferase. Within a molar ratio of Hsp33 to luciferase from zero to one through five to one, a linear relationship existed between the amount of Hsp33 present in the activity assay and the extent of the suppression of aggregation (Figure 1). This concentration range was sufficient to analyze the reactivation kinetics of Hsp33 in detail.

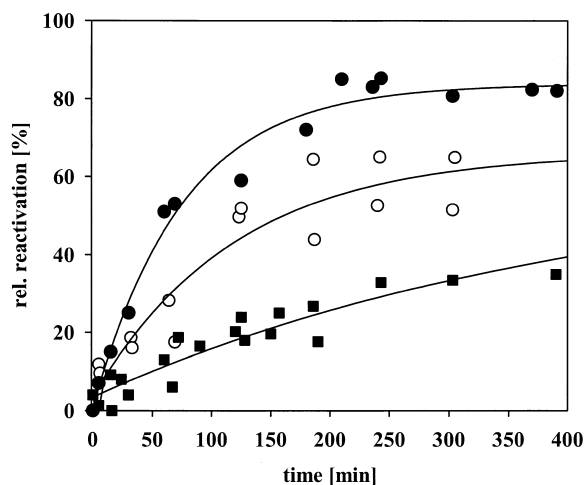


Figure 2. Reactivation of Hsp33 is a Concentration-Dependent Process

Reduced, zinc-reconstituted Hsp33 was incubated in the presence of 2 mM  $H_2O_2$  at 43°C. The concentration of Hsp33 in the incubation reaction was either 5  $\mu M$  (solid square), 50  $\mu M$  (open circle), or 200  $\mu M$  (solid circle). At defined time points after the start of the incubation, aliquots were taken and added to the activity assay (final concentration of 240 nM). Then, denatured luciferase (final concentration of 48 nM) was added, and the light scattering signal after 6 min of incubation was recorded. The light scattering signal in the presence of 240 nM inactive, cysteine-free mutant was taken as 0% activity, while the light scattering signal in the presence of 240 nM active Hsp33DCCSSS mutant was taken as 100% activity.

### Reactivation of Hsp33's Chaperone Function is Concentration Dependent

To analyze the reactivation kinetics of Hsp33, reduced and zinc-reconstituted Hsp33 were prepared [5]. Samples of 5  $\mu M$ , 50  $\mu M$ , and 200  $\mu M$  Hsp33 were reactivated at 43°C in the presence of 2 mM  $H_2O_2$ . The kinetics of the reactivation were monitored by analyzing Hsp33's influence on the aggregation of renaturing firefly luciferase. The Hsp33 concentration used in the luciferase activity assay was in a 5-fold molar excess relative to luciferase (0.24  $\mu M$ ) and thus was independent of the Hsp33 concentration used in the Hsp33 reactivation reactions.

Figure 2 shows that the reactivation reaction of Hsp33 is a concentration-dependent process. The apparent half time ( $T_{1/2}$ ) of reactivation using 5  $\mu M$  Hsp33 protein was more than 120 min, but the apparent half time was only 52 min when 200  $\mu M$  Hsp33 protein was reactivated. In both cases, the second reactant,  $H_2O_2$ , was present in a large excess in the reaction. Furthermore, the net yield of the reactivated species increased with increasing protein concentration. These results suggested that dimerization of Hsp33, as observed in the crystal structure of the chaperone [1] might indeed be involved in the activation process of Hsp33.

### Activation Step 1: Disulfide Bond Formation and Zinc Release

Hsp33's oxidation-induced reactivation is initiated by the formation of two intramolecular disulfide bonds connecting the two neighboring cysteines Cys232-Cys234

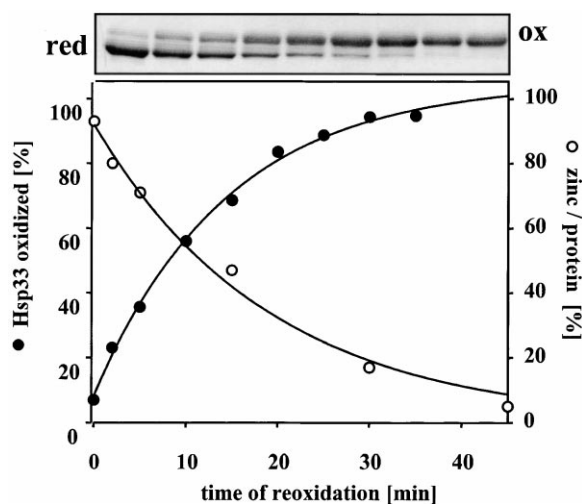


Figure 3. Zinc Release of Hsp33 Parallels Disulfide Bond Formation

Reduced, inactive Hsp33 (50  $\mu M$ ) was incubated in the presence of 2 mM  $H_2O_2$  at 43°C. At defined time points after the start of the incubation, aliquots were taken. To determine the kinetics of zinc release (open circle), the PAR/PMPS assay was performed. To analyze the kinetics of disulfide bond formation (solid circle), AMS thiol trapping was performed. The AMS-treated protein samples were loaded onto a 14% NOVEX SDS-PAGE gel (upper panel), and the intensity of the bands was determined using densitometry. The reactions followed pseudo-first order kinetics and were fitted accordingly.

and Cys265-Cys268 [2, 6]. This process leads to the release of the zinc atom that is coordinated by the four conserved cysteines in reduced Hsp33. To analyze whether the concentration-dependent reactivation of Hsp33 parallels disulfide bond formation or reflects an additional step in the reactivation process of Hsp33, the kinetics of disulfide bond formation and zinc release were analyzed. Formation of intramolecular disulfide bonds can be monitored by thiol-trapping methods that allow the separation and visualization of oxidized and reduced species on polyacrylamide gels (Figure 3, upper panel). We made use of a method that we have previously established to monitor the disulfide status of Hsp33 both in vitro and in vivo [2]. In short, we first alkylate all accessible thiol groups in Hsp33 with the fast-acting reagent iodoacetamide. After removal of excess iodoacetamide, disulfide bonds present in the protein are reduced with DTT. In the final step, the thiol groups previously engaged in disulfide bonds in the oxidized protein are alkylated with 4-acetamido-4'-maleimidylstilbene-2,2'-disulfonic acid (AMS). AMS is a thiol reactive reagent that alkylates cysteines, thereby adding 500 Da molecular mass per thiol group. Completely oxidized Hsp33 contains two disulfide bonds and shows, therefore, a slower mobility on SDS-PAGE gels due to the addition of four AMS molecules. This translates into a 2 kDa change in molecular mass (Figure 3, upper panel). Incubation of 50  $\mu M$  reduced Hsp33 in 2 mM  $H_2O_2$  at 43°C led to the rapid formation of oxidized Hsp33. After 30 min of incubation, Hsp33 had almost completely shifted into the higher migrating, oxidized species (Figure 3, upper panel). The mobility difference between the oxidized and reduced species correlated

well with the addition of 2 kDa in the oxidized form by the modifying agent and suggested the simultaneous formation of both disulfide bonds. Only a very faint band migrating between the oxidized and reduced species was noticeable. This most likely represents a small subpopulation of Hsp33, with only one disulfide bond formed. The apparent half time of disulfide bond formation under these conditions was calculated to be  $\sim 11$  min (Figure 3). A very similar apparent half time of  $T_{1/2} = 13 \pm 2$  min was determined when the oxidation-induced zinc release was analyzed using the PAR/PMPS assay (Figure 3). A comparison of both time courses revealed that the formation of the two disulfide bonds very closely matches the kinetics determined for the zinc release. Interestingly, the oxidation rate was significantly faster than the rate of reactivation of 50  $\mu\text{M}$  Hsp33 in which an apparent half time of about 82 min was calculated (Figure 2). This result suggests that disulfide bond formation and oxidative zinc release is necessary for and precedes the complete reactivation of Hsp33.

#### Disulfide Bond Formation and Zinc Release is Concentration Independent

Disulfide bond formation in Hsp33 was significantly faster than Hsp33's reactivation reaction. This suggests that there is an additional step in the reactivation reaction in which the rate-determining step of the activation occurs after disulfide bond formation. The dependence of Hsp33's reactivation rate and yield on the concentration of Hsp33 suggested that a second order reaction is involved in Hsp33 reactivation. To ascertain that the concentration dependence is not due to limiting amounts of  $\text{H}_2\text{O}_2$  in the reaction, the dependence of Hsp33 disulfide bond formation on the Hsp33 concentration was analyzed. We showed in Figure 3 that the zinc release exactly parallels disulfide bond formation. This allowed us to use the analysis of zinc release from increasing concentrations of Hsp33 upon addition of  $\text{H}_2\text{O}_2$  as an indirect way to monitor disulfide bond formation. The zinc release from Hsp33 by oxidation showed no concentration dependence. The apparent half time of the zinc release was in the same order of  $13 \pm 2$  min, independent of the protein concentration (5–200  $\mu\text{M}$ ) used in the incubation reaction. These data suggested a model in which the oxidative reactivation of Hsp33 involves at least two consecutive reactions: first, the fast formation of two disulfide bonds (Cys232-Cys234 and Cys265-Cys268), which leads to the complete release of zinc and second, the rate-determining step of the activation process, which is protein concentration dependent and results in a highly active molecular chaperone.

#### Activation Step 2: Dimerization of Hsp33

The structure of Hsp33 that shows Hsp33 in dimeric conformation as well as the dependence of Hsp33's reactivation reaction on the protein concentration suggested that oligomerization was indeed part of Hsp33's activation process. To analyze the potential changes in the oligomerization state of Hsp33 upon oxidation and activation, analytical ultracentrifugation experiments

were performed. A strict correlation was established between the activity of Hsp33 and the oligomerization state of the protein (Figure 4a). The cysteine-free, inactive Hsp33 mutant sedimented as a monomer with an apparent  $s$  value of  $s(\text{app}) = 1.86$  S, very similar to the one obtained for the reduced and inactive wild-type protein. To confirm the monomeric character of reduced, inactive wild-type Hsp33, sedimentation equilibrium analysis was performed and revealed a molecular mass of  $M_r = 30,070$ . In contrast, a substantially higher sedimentation velocity was observed for the reactivated, oxidized wild-type Hsp33 as well as the highly active Hsp33DCCSSS mutant. At protein concentrations of 0.2 mg/ml, the  $s$  values were calculated to be 2.75 S and 2.69 S, respectively, indicating that the majority of active Hsp33 is present as dimers in solution. The association was strongly dependent on the protein concentration, with an increase in dimer formation occurring upon raising the Hsp33 concentration. These results were in excellent agreement with the activity of the respective protein preparations (Figure 4a) and clearly demonstrated that the concentration-dependent step in Hsp33's reactivation reaction involves the association of two oxidized monomers to the highly active dimer. Analysis of the dependence of the sedimentation velocity on the Hsp33 protein concentration revealed a dissociation constant,  $K_D$ , of 0.6  $\mu\text{M}$  (Figure 4b). This is well within the range of Hsp33's physiological protein concentration, which was calculated to be about 2–3  $\mu\text{M}$  Hsp33 under nonstress conditions [2]. Dimerization of Hsp33 will be even more favored under stress conditions, in which the steady state level of the Hsp33 protein increases at least 2-fold upon a temperature shift from 30°C to heat shock temperatures (45°C).

#### Conformational Changes during the Activation Process of Hsp33

Activation and oligomerization of proteins is often accompanied by considerable structural rearrangements that can be monitored using spectroscopic techniques such as protein fluorescence. If aromatic amino acids like tyrosine and tryptophan residues are located in areas of major rearrangements, changes in relative fluorescence or, in the case of tryptophan residues, changes in the wavelength of the emission maximum are often observed [14]. A comparison of the fluorescence properties of reduced, inactive Hsp33 versus oxidized, activated Hsp33 suggested major structural rearrangements upon the activation process of Hsp33 (Figure 5a). Activated wild-type protein showed significantly quenched tyrosine fluorescence at 303 nm and a substantially broadened fluorescence spectrum that suggested an increased energy transfer between tyrosine and tryptophan residues. The extent of conformational changes in the protein fluorescence of Hsp33 upon activation was nicely reflected by the fluorescence ratio at 306 and 330 nm. Upon activation of the protein, this ratio changed by an impressive 25%, from 1.0 to less than 0.75 in the oxidized, active protein. It is noteworthy that a tyrosine fluorescence quench was also detectable in the cysteine-free Hsp33 mutant, suggesting that part of the enhanced tyrosine

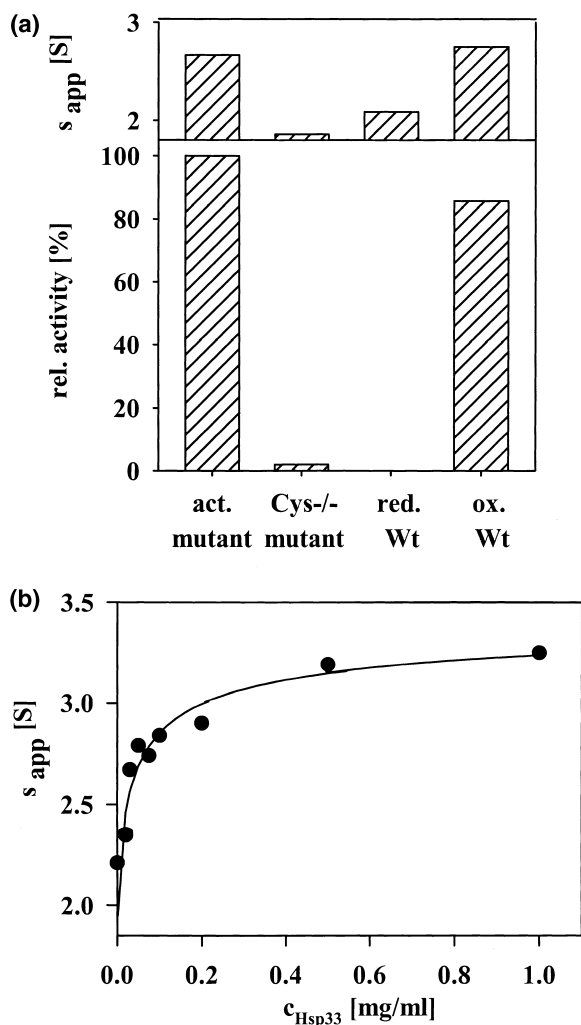


Figure 4. Active Hsp33 is a Dimer in Solution

(a) Correlation between the activity of various Hsp33 preparations and their oligomerization states. The activities of the highly active Hsp33DCCSSS; the cysteine-free, inactive Hsp33 mutant; the reduced zinc-reconstituted wild-type Hsp33; and the reoxidized wild-type Hsp33 were determined as described in Figure 2. The identical protein preparations were then used for analytical ultracentrifugation experiments. The  $s$  values for the individual proteins were determined at 40,000 rpm using a protein concentration of 0.2 mg/ml.

(b) The monomer-dimer equilibrium of oxidized Hsp33. Reduced, zinc-reconstituted Hsp33 (200  $\mu$ M in 40 mM HEPES [pH 7.5]) was reoxidized by the addition of 2 mM  $H_2O_2$  and incubation for 3 hr at 43°C. Subsequently, the protein solution was diluted with 40 mM HEPES-KOH (pH 7.5) to protein concentrations ranging from 25  $\mu$ g/ml to 1 mg/ml. The dependence of the apparent  $s$  values on the protein concentration was measured at 40,000 rpm and analyzed according to a monomer-dimer equilibrium. The solid line represents a fit to a dissociation constant of  $K_D = 5.9 \times 10^{-7}$  M.

fluorescence in reduced wild-type Hsp33 might be due to the formation of the zinc binding domain. Hsp33 has nine tyrosines, with Tyr267 being located between the Cys265-Cys268 pair. This tyrosine residue could be partly responsible for the increased tyrosine fluorescence that is detectable in the reduced wild-type protein. Additional conformational changes, however, seem

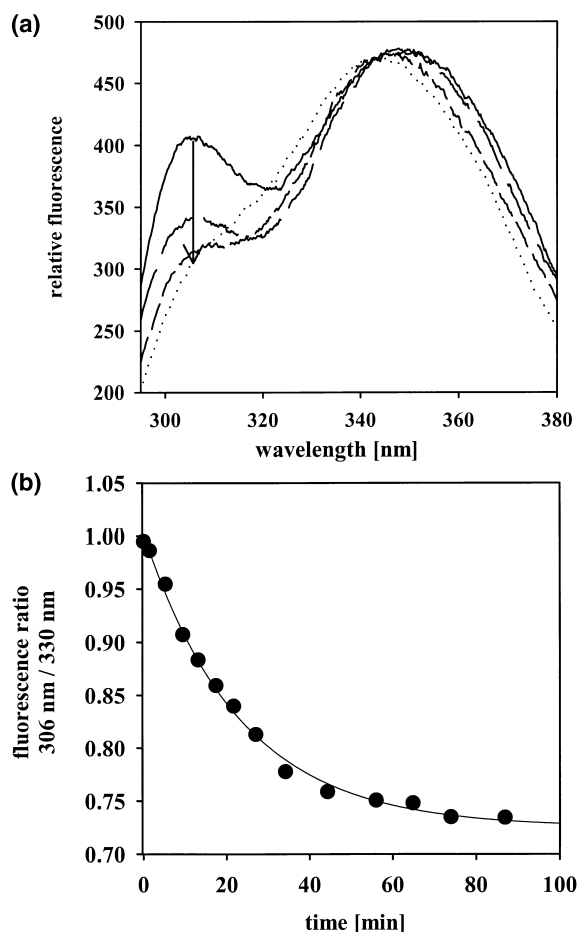


Figure 5. Conformational Changes of Hsp33 upon Oxidation and Zinc Release

(a) The fluorescence spectra of reduced, zinc-reconstituted wild-type Hsp33 (solid line); cysteine-free, inactive Hsp33 mutant (long dashed line); highly active Hsp33DCCSSS mutant (short dashed line); and reoxidized wild-type Hsp33 (dotted line) (3  $\mu$ M each in 40 mM HEPES-KOH [pH 7.5]). The excitation wavelength was set to 285 nm.

(b) Tyrosine fluorescence quench accompanies disulfide bond formation and zinc release. Reduced and zinc-reconstituted Hsp33 (50  $\mu$ M) was incubated in the presence of 2 mM  $H_2O_2$  at 43°C. At defined time points after the start of the incubation, aliquots were taken and diluted into 40 mM HEPES-KOH (pH 7.5) (final concentration of 3  $\mu$ M). Then, fluorescence spectra were recorded as described in Figure 5a, and the ratio of relative fluorescence at 306 nm and 330 nm was determined. The reaction followed pseudo-first order kinetics and was fitted accordingly. The same  $T_{1/2}$  was obtained when 5  $\mu$ M Hsp33 protein was reactivated and fluorescence spectra of 0.83  $\mu$ M Hsp33 were monitored.

likely to occur since the difference between the reduced wild-type protein and the cysteine-free mutant accounted for less than 15% of the 25% total fluorescence change.

If zinc binding was indeed responsible for the increased tyrosine fluorescence that is detectable in the reduced wild-type protein, determination of the fluorescence changes upon oxidation of Hsp33 should reveal very similar kinetics to the ones obtained for disulfide

bond formation and zinc release. If dimerization played into this fluorescence change as well, the reaction should become concentration dependent, and two distinct rate constants should be detectable. Therefore, fluorescence measurements were performed during the reactivation reaction of Hsp33 (Figure 5b). For the reactivation reaction, 5 or 50  $\mu\text{M}$  reduced and zinc-reconstituted Hsp33 was incubated in the presence of 2 mM  $\text{H}_2\text{O}_2$  at 43°C. At defined time points after the start of the incubation, aliquots were taken, and fluorescence spectra were recorded. Independent of the Hsp33 concentration that was present in the reactivation reaction, the apparent half time of the fluorescence change was calculated to be  $15 \pm 0.3$  min (Figure 5b). The fluorescence change covered the total amplitude, excluding the possibility of a significantly slower, second reaction, and suggested conformational changes that are independent of zinc coordination. These results were in excellent agreement with the apparent half times of disulfide bond formation and zinc release that were determined under similar conditions (Figure 3). From these experiments, we concluded that the first step of Hsp33's reactivation process is accompanied by significant structural rearrangements in Hsp33, which lead to the formation of a dimerization-competent, oxidized Hsp33 monomer. This was also confirmed by analyzing the secondary structure of Hsp33 by performing circular dichroism measurements (data not shown).

In an attempt to directly visualize the dimerization process of Hsp33, we made use of a tyrosine residue (Tyr127) that has been shown in the crystal structure to be located at the dimer interface near the bottom of the  $\beta 7$  strand (Figure 6a). The  $\beta 7$  strands from both Hsp33 monomers meet and form the saddle-shaped continuous  $\beta$  sheet in Hsp33, one of the two putative substrate binding regions in Hsp33. In the dimer, Tyr127 is embedded in the hydrophobic environment of the dimer-dimer interface, mainly due to the close contact with Tyr145 from the other molecule (Figure 6a). Based on our working model, we predicted that Tyr127 would be exposed to the polar environment whenever Hsp33 was present as a monomer. Since Hsp33's sequence harbors numerous tyrosine residues but only one exposed tryptophan residue, we decided to replace Tyr127 with the environmentally more sensitive tryptophan [14]. This probe should allow us to directly monitor the concentration-dependent association of the two monomers. As shown in Figure 6b, significant differences were indeed observed in the tryptophan fluorescence of the reduced and oxidized Hsp33Y127W mutant. While reduced Hsp33Y127W showed an emission maximum of fluorescence at a wavelength similar to reduced wild-type Hsp33 (Figure 5a), oxidized Hsp33Y127W showed a more than 6 nm blueshift in the wavelength of the emission maximum. This confirmed our working model and suggested that Trp127 is exposed in the monomer and becomes buried in the hydrophobic environment of the extended  $\beta$  sheet upon the dimerization of Hsp33 (Figure 6a). Moreover, the oxidation-induced quench in tyrosine fluorescence was also noticeable in the active form of the Hsp33Y127W mutant protein, allowing us now to very conveniently visualize the kinetics of disulfide bond formation and dimerization at the same time (Figure 6c).

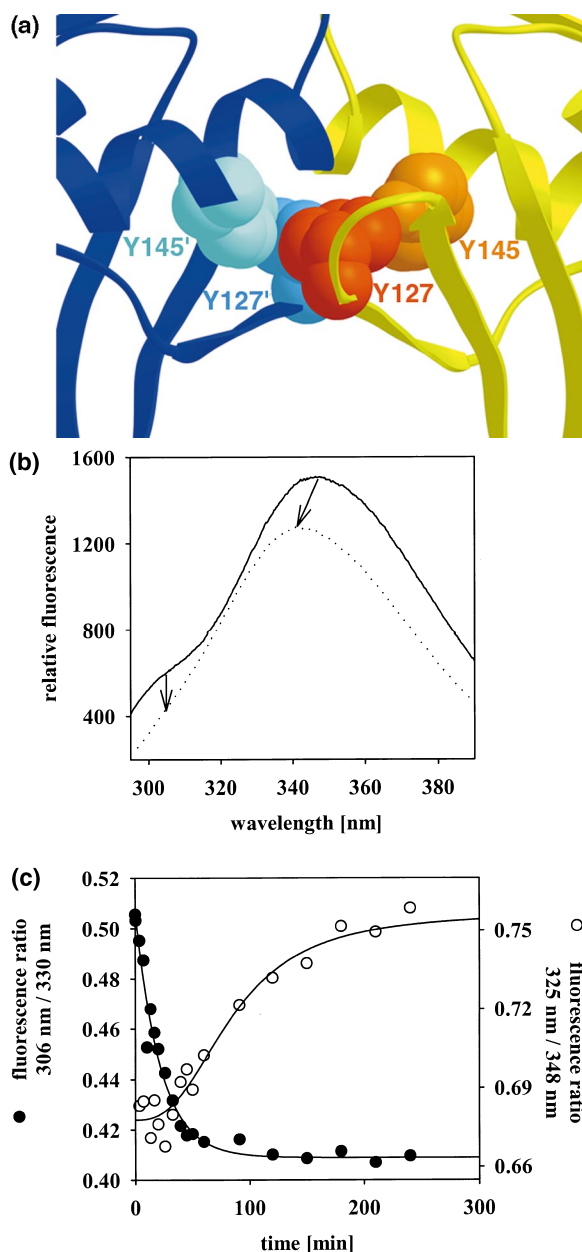


**Figure 6. Monitoring the Dimerization Process of Hsp33**  
(a) The hydrophobic dimerization interface in the core region (aa 1–178) of Hsp33. Upon dimerization of Hsp33, Tyr127 of molecule A (yellow ribbon) comes in close proximity to Tyr145' of molecule B (blue ribbon), and Tyr127' of molecule B comes in close proximity to Tyr145 of molecule A.  
(b) The fluorescence properties of reduced (solid line) and oxidized (dotted line) Hsp33Y127W mutant protein. The protein concentration was 5  $\mu\text{M}$  in 40 mM HEPES-KOH (pH 7.5). The excitation wavelength was 285 nm.  
(c) Oxidation and dimerization of Hsp33. Reduced and zinc-reconstituted Hsp33Y127W mutant protein (50  $\mu\text{M}$ ) was incubated in the presence of 2 mM  $\text{H}_2\text{O}_2$  at 43°C. At defined time points after the start of the incubation, aliquots were taken and diluted into 40 mM HEPES-KOH (pH 7.5) (final concentration of 5  $\mu\text{M}$ ). Then, fluorescence spectra were recorded as described in Figure 5a. To monitor oxidation (solid circle), the ratio of relative fluorescence at 306 nm and 330 nm was determined. The reaction followed pseudo-first order kinetics and was fitted accordingly. To determine the kinetics of the dimerization reaction (open circle), the ratio of relative fluorescence at 325 and 348 nm was determined.

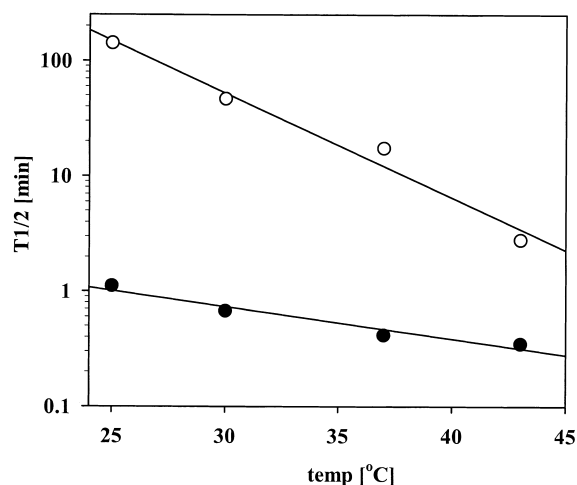


Figure 7. Reactivation of Hsp33 is a Highly Temperature-Dependent Process

Reduced and zinc-reconstituted Hsp33 (50  $\mu$ M) was incubated in the presence of 50  $\mu$ M CuCl<sub>2</sub> and 2 mM H<sub>2</sub>O<sub>2</sub> at the indicated temperatures. At defined time points after the start of the incubation reaction, aliquots were taken, and either the T<sub>1/2</sub> of zinc release (solid circle) was determined as described in Figure 3 or the T<sub>1/2</sub> of the reactivation reactions (open circle) were determined as described in Figure 2.

Reduced, zinc-reconstituted Hsp33Y127W mutant protein (50  $\mu$ M) was reactivated in the presence of 2 mM H<sub>2</sub>O<sub>2</sub> at 43°C, and fluorescence spectra were recorded during the incubation process. As shown in Figure 6c, the tyrosine fluorescence quench reflecting the first step of Hsp33's activation process followed the same kinetic and showed a half time (T<sub>1/2</sub> = 15 min) identical to the one observed for the wild-type protein (Figure 5b). The change in tryptophan fluorescence, however, followed a classical consecutive reaction with an initial lag phase and a subsequent increase in fluorescence. This reaction was dependent on the protein concentration and showed an apparent half time of ~88 min at 50  $\mu$ M (Figure 6c). This was very similar to the apparent half time determined for the reactivation reaction of 50  $\mu$ M Hsp33 (Figure 2) and confirmed that the rate-limiting step in the reactivation reaction of Hsp33 is indeed the formation of the active Hsp33 dimer.

#### Activation of Hsp33's Chaperone Function is Highly Temperature Dependent

Structural rearrangements such as dimerization can be very temperature-dependent processes, depending on the character of the interactions involved [15]. To analyze the temperature dependence of Hsp33's reactivation rate, 50  $\mu$ M reduced and zinc-reconstituted Hsp33 were incubated in 2 mM H<sub>2</sub>O<sub>2</sub> at various temperatures, ranging from 23°C to normal physiological temperatures (30–37°C) to heat shock temperatures (43°C). All reactivation reactions were supplemented with 50  $\mu$ M CuCl<sub>2</sub>. This increased the amount of hydroxyl radicals in the solution and dramatically increased the rate of Hsp33's reactivation process [5] without changing the overall mechanism of the reactivation reaction. The two-step mechanism of Hsp33's reactivation reaction became

particularly obvious at low temperatures (Figure 7). At 23°C, a T<sub>1/2</sub> of 1.2 min was determined for disulfide bond formation and zinc release, while a 100-fold larger value of a T<sub>1/2</sub> of 120 min was determined for the reactivation reaction. At heat shock temperatures, however, the rate of reactivation (T<sub>1/2</sub> = 2.8 min) approached the rate of the zinc release (T<sub>1/2</sub> = 0.4 min). This was mainly due to the extreme increase in the rate of dimerization. The temperature dependence can be expressed as a Q<sub>10</sub> value, which is the rate increase upon a 10°C temperature increase [16]. The majority of noncatalyzed reactions show a Q<sub>10</sub> of about 2, indicating that the reaction rate doubles for each 10 degree increase in temperature [16]. While disulfide bond formation and zinc release showed the expected Q<sub>10</sub> of 2 (Figure 7), the Q<sub>10</sub> of the reactivation rate was more than 7 (Figure 7). This indicated that the dimerization reaction of Hsp33 is an exquisitely temperature-dependent process. That this was independent of the presence of additional CuCl<sub>2</sub> in the incubation reaction became evident when the temperature dependence was analyzed in the absence of additional CuCl<sub>2</sub> and resulted in very similar Q<sub>10</sub> values (data not shown). The significant temperature dependence of Hsp33's dimerization process led to a half time of Hsp33's reactivation reaction of less than 2.8 min under heat shock conditions in vitro (Figure 7). Since Hsp33's high chaperone activity depends on the dimer formation, temperature could, therefore, be considered to play an additional role in the regulation of Hsp33's chaperone activity. Interestingly, the molecular chaperone Hsp26, which is a member of the ATP-independent family of small heat shock proteins (sHsp), has recently been found to use a similar concept [17]. However, in contrast to Hsp33, in which increased temperature leads to an increase in active dimer formation by promoting the association of oxidized, less active monomers, Hsp26 shows an increase in active dimer formation by promoting the dissociation of less active, large Hsp26 oligomers [17].

The greatly accelerated dimerization reaction of Hsp33 at elevated temperatures suggested the involvement of major structural rearrangements, including numerous hydrophobic interactions, which might initiate and support the dimer formation. The crystal structure of dimeric Hsp33 revealed a number of interfaces harboring hydrophobic interactions that might play a role in driving the dimerization under heat shock conditions [1]. These were found between residues of the two adjacent  $\beta$ 7 strands, the strands shown to build the interface within the saddle-shaped  $\beta$  sheet (Figure 6a), as well as in the domain-swapped region in which extensive hydrophobic interactions exist between the apical four-stranded  $\beta$  sheet of the one molecule and the  $\alpha$  helices from the domain-swapped C-terminal domain of the other molecule. Several highly conserved, hydrophobic amino acids are present in this interface and are likely to guide and stabilize the domain swapping and dimer formation. In our model, oxidation-induced disulfide bond formation, and in particular the formation of the Cys232-Cys234 disulfide bond, might initiate the structural rearrangement of the C-terminal domain in Hsp33. This is plausible considering that disulfide bond formation between two cysteines, which are separated by only one amino acid, such as those found in Hsp33's

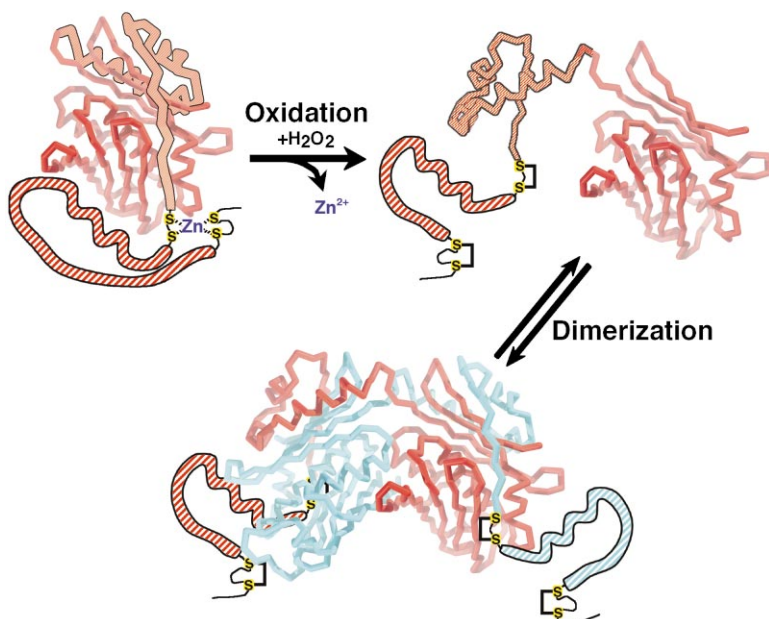


Figure 8. Schematic Model of Hsp33 Dimerization and Activation Derived from Structural and Solution Results

Zinc-reconstituted, reduced Hsp33 forms a stable monomer in solution and is inactive as a molecular chaperone. The zinc binding carboxy-terminal domain of Hsp33 may block the substrate binding site and/or the dimerization interface. Upon incubation in  $H_2O_2$ , two intramolecular disulfide bonds form, and zinc is released. This leads to both conformational changes in the protein and partial chaperone activity. In a concentration-dependent process, two oxidized monomers (colored in cyan and red) associate and form a highly active Hsp33 dimer. The four conserved cysteines that ligand the zinc in reduced Hsp33 and form disulfide bonds in the oxidized form of Hsp33 are highlighted in yellow. The modeled regions are drawn as hatched tubes. The solid tubes show the Hsp33 structure as solved by Vijayalakshmi et al. [1].

$Cys_{232}$ -X- $Cys_{234}$  motif, can cause a change in main chain direction and distorted bond angles [18]. Evidence supporting the idea that the  $Cys_{232}$ - $Cys_{234}$  disulfide bond is indeed the crucial disulfide bond for Hsp33's chaperone activity and dimer formation came from the finding that Hsp33 mutants that are missing the second disulfide bond are fully active and dimeric when oxidized.

#### Activity of the Oxidized Hsp33 Monomer

The activity of a molecular chaperone, and in particular, the affinity for certain folding intermediates, depends on the binding site of the chaperone and on the folding state of the respective substrate protein. For example, the extent of substrate binding to the chaperones of the small heat shock protein family is considered to be "unique for a given protein" and is largely determined by the exposure of structural elements recognized by the chaperones [19]. These structural elements that are recognized by molecular chaperones are considered to be mostly of a hydrophobic nature, normally buried in the interior of the protein and only transiently exposed during folding and stress-induced unfolding processes [13]. The hydrophobic pendants, usually small grooves [20] or patches [21] on the surface of chaperones, have been found to function as suitable substrate binding sites. Therefore, increasing the extent of hydrophobic surfaces on folding intermediates or within the substrate binding site of the chaperone will dramatically increase the affinity and stability of chaperone-substrate interactions. This appears to be the mechanism by which ATP-independent Hsp40 regulates its chaperone activity [22]. Cyr and coworkers [22] recently demonstrated that dimerization of the two Hsp40 monomers is required for Hsp40's high substrate binding affinity. This might be due to the peptide binding site on one monomer being insufficient for stable interactions with protein folding intermediates [22]. A very similar concept appears to apply for the redox-regulated heat shock protein Hsp33.

Disulfide bond formation and dimerization seem to cause different conformational changes in Hsp33. This allows different substrate proteins to interact with Hsp33 at different stages during the activation process. For Hsp33, to interact with and prevent the aggregation of highly structured, thermally unfolding luciferase, formation of the oxidized monomer appears to be sufficient [2]. Using these early unfolding intermediates as substrates, activation of Hsp33's chaperone function has been shown to parallel oxidation-induced zinc release [2]. Analysis of Hsp33's influence on completely unfolded, highly aggregation-sensitive proteins like chemically denatured luciferase, on the other hand, revealed that Hsp33 needs to dimerize in order to efficiently compete against the otherwise irreversible aggregation process. It appears that these additional conformational rearrangements that accompany dimer formation are required for the increased affinity to the substrate proteins. Analysis of the crystal structure of Hsp33 revealed the presence of two putative substrate binding sites extending over and involving both monomers [1]. These sites provide large noncharged, nonpolar surfaces capable of interacting via hydrophobic interactions with various substrate proteins. These surfaces are likely to be smaller and, therefore, less efficient in the oxidized monomer. Preliminary functional analysis of Hsp33 mutant proteins that are defective in dimerization revealed an  $\sim 8\times$  lower affinity of these mutants for chemically denatured luciferase (data not shown). Mutational analyses are now underway to determine the substrate binding region in the oxidized Hsp33 monomer as well as in the highly active dimer.

#### Biological Implications

The molecular chaperone Hsp33 is a novel, redox-regulated protein. Activation of Hsp33's chaperone function helps cells to survive oxidative stress conditions. Our



biochemical studies in combination with the crystal structure of Hsp33 [1] allowed us to draw a model, as shown in Figure 8, detailing the highly sophisticated activation process of Hsp33. Under normal conditions, Hsp33 is kept in an inactive, monomeric state. This conformation of Hsp33 is stabilized and maintained in a primed to be activated state by the formation of a high affinity zinc center. We suspect that the zinc binding domain of Hsp33 is in part masking the dimerization sites and/or the putative substrate binding sites. Upon oxidative stress, two disulfide bonds form, and the zinc is released. This causes major structural rearrangements in the protein and the partial activation of Hsp33's chaperone activity. To obtain a fully activated molecular chaperone, dimerization of two oxidized monomers is necessary. This association reaction is both concentration- and highly temperature-dependent; optimized for a molecular chaperone that is overexpressed under heat shock conditions. Dimerization causes the formation of two large, putative substrate binding sites in Hsp33 that are highly efficient in protecting folding proteins from irreversible aggregation processes.

## Experimental Procedures

### Hsp33 Mutants

The cysteine mutants in the gene for Hsp33 were constructed using the Quickchange side specific mutagenesis system (Stratagene). To simplify our mutant nomenclature, only the identities of the respective cysteine residues are given. Hsp33 contains six cysteines at positions 141, 232, 234, 239, 265, and 268, with cysteines 141 and 239 being nonconserved and dispensable [2, 5]. The remaining cysteine residues act to form two disulfide bonds (Cys 232-Cys234 and Cys265-Cys268) in the oxidized, active form of Hsp33 or chelate zinc in the reduced, inactive form. Thus, the mutant DCCCC has the nonessential cysteine Cys141 mutated to aspartic acid (D) and the remaining cysteines left intact. CCCSCC has the fourth cysteine, Cys239, mutated to serine (S), and the mutant DCCSCC has both of the nonessential cysteines changed to aspartic acid (D) or serine (S), respectively [2]. This double mutant *hsp33Cys141D-239S*, which has been cloned into the expression vector pET11a (pEM3) [2], was used as a template for all the subsequent mutagenesis reactions. The forward and respective antiparallel primers C265S-C268S were used to generate *hsp33C141D-239S-265S-268S*, which had four of the six cysteines replaced. The purified Hsp33DCCSSS mutant protein was shown to be fully active in vitro and is referred to as the active mutant. The plasmid encoding this active mutant (pJH5) was subsequently used as a template to construct the cysteine-free mutant *hsp33C141D-C232S-C234S-C239S-C265S-C268S* (pJH6) in which all six cysteines had been replaced. The purified mutant protein Hsp33DSSSSS was shown to be constitutively inactive in vitro and is referred to as the inactive mutant.

The forward primers that were used are as follows:

C232S-C234S: 5' CGATCCG CAGGATGTGGAGTTC A AATCGACTA GTTCGCGT GAACGTCCGCGGATGCGC3'

C265S-C268S: 5' CCTGGCGGAAGATGGCGAAATTGACATGCA TTC TGATTACT CCGGTAACCACTATCTGTTCAATGCGATGGATATTGC3'.

To construct the tyrosine 127 to tryptophan mutant *hsp33Y127W* in pET11a (pKT1), wild-type *hsp33* cloned into pET11A (pUJ30) was used as template DNA [2]. The forward and respective antiparallel primer Y127W that was used for introducing the mutations is as follows:

Y127W: 5' GCGAAGGCGAACGCTGGCAGGCGTAGTAGGCCCTGG AAGG3'

All introduced mutations were confirmed by sequencing. For protein expression, the plasmids were transformed into a BL21 strain that contained a deletion of the *hsp33* gene (JH13). To generate the *hsp33* deletion strain JH13, the *hsI/O::Km* mutant allele [2] was

moved using P1 transduction into the BL21 strain by selecting for  $km^R$  resistance. *hsI/O* is the name for the *hsp33* gene. The *hsp33::Km* allele is an internal deletion-substitution mutation in which the kan resistance cassette replaces 737 bp of the *hsp33* gene.

Strains containing the *hsp33* mutant overexpressing plasmids were grown in LB medium supplemented with 1 mM  $ZnCl_2$ . Hsp33 protein expression was induced by the addition of IPTG to 1 mM, and the purification of the Hsp33 mutant proteins was performed in the absence of reducing agents according to the purification protocol of wild-type Hsp33 [2].

### Preparation of Reduced, Zinc-Reconstituted, and Reoxidized, Active Hsp33

To obtain a homogeneous preparation of reduced and inactive Hsp33, purified Hsp33 at a concentration of 50–200  $\mu M$  was incubated in 2 mM DTT, 20–100  $\mu M$   $ZnCl_2$ , and 40 mM HEPES-KOH (pH 7.5) for 60 min at 37°C. After the incubation, excess DTT and zinc were removed using PD10 (Pharmacia) gel filtration columns that were equilibrated in 40 mM HEPES-KOH (pH 7.5). The protein was eluted with 2 ml 40 mM HEPES-KOH (pH 7.5) and concentrated using Centricon YM-30 concentrators. The protein concentration was determined using the calculated extinction coefficient of 0.545  $mg^{-1}cm^{-1}$  for wild-type Hsp33 [2] and 0.660  $mg^{-1}cm^{-1}$  for the Hsp33Y127W mutant protein [23]. To reactivate reduced and inactive Hsp33, 50 or 200  $\mu M$  zinc-reconstituted Hsp33 was incubated in the presence of 2 mM  $H_2O_2$  at 43°C for 180–240 min.

### Determination of Accessible Thiol Groups in the Active Hsp33DCCSSS Mutant

Accessible thiol groups in purified, untreated and reduced Hsp33DCCSSS were determined in 6 M GdnHCl using Ellmans reagent according to Creighton [24].

### Activity Measurements of Hsp33

To analyze the chaperone activity of Hsp33, Hsp33's influence on the aggregation of refolding luciferase was tested [6]. Firefly luciferase (Hoffmann LaRoche) was denatured to a final concentration of 7.7  $\mu M$  in 4.3 M Gdn<sup>+</sup>HCl for 2 hr at room temperature. To initiate the refolding of luciferase, the unfolded enzyme was diluted 1:160 (final concentration of 48 nM) into 1600  $\mu l$  40 mM HEPES (pH 7.5) at 30°C in the absence or presence of Hsp33. Light scattering was monitored using a Hitachi F4500 fluorimeter equipped with a thermostated cell holder and stirrer. Excitation and emission wavelengths were set to 350 nm, and the excitation and emission slit widths were set to 2.5 nm.

To initiate the activation of Hsp33, reduced, zinc-reconstituted Hsp33 (5, 50 or 200  $\mu M$  in 40 mM HEPES-KOH [pH 7.5]) was incubated in the presence of 2 mM  $H_2O_2$  at 43°C. At defined time points after the addition of  $H_2O_2$ , aliquots were taken and diluted to a final concentration of 0.24  $\mu M$  into the refolding buffer, which was present in the cuvette. Then, denatured luciferase was added, and the light scattering of aggregating luciferase was monitored. To exclude re-activation of Hsp33 by incubation at elevated temperature alone, the activity of Hsp33 was determined after the incubation of Hsp33 in the absence of  $H_2O_2$  for 5 min at 43°C. The light scattering signal, which was reached after 6 min of luciferase incubation in the presence of a 5-fold molar excess of the inactive, cysteine-free mutant, was set to 0% activity. The light scattering signal reached after 6 min in the presence of the highly active mutant Hsp33DCCSSS was set at 100% activity.

To analyze the temperature dependence of Hsp33's reactivation reaction, 50  $\mu M$  reduced, zinc-reconstituted Hsp33 was incubated in 50  $\mu M$   $CuCl_2$  and 2 mM  $H_2O_2$  at 23°C, 30°C, 37°C, or 43°C. At defined time points after the start of the reactivation, aliquots were taken, and the activity was determined as described.

### Thiol Trapping with AMS

Thiol trapping with the thiol-specific reagent 4-acetamido-4'-maleimidylstilbene-2,2'-disulfonic acid (AMS, Molecular Probes) was performed according to Jakob et al. [2]. The protein bands were visualized using a fast, highly sensitive Coomassie blue staining technique [25]. Proteins that migrated slower after the AMS treatment represent the oxidized form. To determine the rate of oxidation, the inten-

sities of the individual bands were analyzed using densitometry (Beckman).

#### Oxidation-Induced Zinc Release of Hsp33

Reduced and zinc-coordinated Hsp33 (5, 50, or 200  $\mu$ M in 40 mM HEPES-KOH [pH 7.5]) was incubated in the presence of 2 mM  $H_2O_2$  at 43°C. At defined time points after the start of the reoxidation, aliquots were taken (3–5  $\mu$ M), and the cysteine-coordinated zinc was determined using the PAR/PMPS assay [26] according to Jakob et al. [5]. To analyze the temperature dependence of Hsp33's oxidation reaction, 50  $\mu$ M reduced, zinc-reconstituted Hsp33 was incubated in 50  $\mu$ M  $CuCl_2$  and 2 mM  $H_2O_2$  at 23°C, 30°C, 37°C, or 43°C. At defined time points after the start of the reactivation, aliquots were taken, and the zinc release was determined [5].

#### Analytical Ultracentrifugation

Analytical ultracentrifugation measurements were performed at a XL-A centrifuge (Beckman) using an AN50Ti rotor and double sector cells. Sedimentation equilibrium (10,000 rpm) and sedimentation velocity (40,000 rpm) experiments were monitored at 20°C using wavelengths of 230 and 280 nm, respectively. The various Hsp33 preparations included the cysteine-free inactive Hsp33 mutant, the highly active Hsp33DCCSSS mutant, reduced and zinc-reconstituted wild-type Hsp33, and reoxidized wild-type Hsp33. For the reoxidation of Hsp33, 50 or 200  $\mu$ M reduced, zinc-reconstituted Hsp33 was incubated in the presence of 2 mM  $H_2O_2$  at 43°C for 180 min. The sedimentation analysis was performed with a protein concentration of 0.2 mg/ml in 40 mM HEPES-KOH (pH 7.5) buffer. The apparent values of the molecular mass and the sedimentation velocity were calculated using the software provided by Beckman Instruments. The dependence of the apparent *s* value on the protein concentration was analyzed according to Luther et al. [27], assuming a monomer-dimer equilibrium.

#### Spectroscopic Analysis

Hsp33's fluorescence properties were analyzed using a Hitachi F4500 fluorimeter. The excitation wavelength was set to 285 nm, and emission spectra were recorded from 295 nm to 380 nm. The emission slit widths and excitation slit widths were set to 5 nm and 10 nm, respectively. The temperature was set to 25°C. The Hsp33 preparations that were analyzed included the cysteine-free inactive Hsp33 mutant, reduced and zinc-reconstituted wild-type Hsp33, the active Hsp33DCCSSS mutant, and reoxidized wild-type Hsp33 (final concentration of 3  $\mu$ M in 40 mM HEPES-KOH [pH 7.5]). To determine the fluorescence properties of the Hsp33Y127W mutant, reduced and zinc-reconstituted as well as reoxidized mutant protein was prepared. Hsp33Y127W mutant protein was diluted to a final concentration of 5  $\mu$ M in 40 mM HEPES-KOH, and fluorescence spectra were recorded as described.

To analyze fluorescence changes in wild-type Hsp33 and Hsp33Y127W upon reoxidation, 50  $\mu$ M reduced and zinc-reconstituted Hsp33 protein was incubated in the presence of 2 mM  $H_2O_2$  at 43°C. At defined time points after the start of the incubation, aliquots were taken, diluted into 40 mM HEPES-KOH (pH 7.5) to a final protein concentration of 3 or 5  $\mu$ M, respectively, and analyzed as described. The ratio of relative fluorescence at 306 nm and 330 nm, and in the case of Hsp33Y127W, the ratio between 325 nm and 348 nm was calculated. The same experiments were also performed with 5  $\mu$ M wild-type protein and 5 or 200  $\mu$ M Hsp33Y127W mutant protein present at the time of the reactivation reaction.

#### Acknowledgments

We thank Alexandra Megner and Srinivas Sridhara for their excellent technical assistance. This work was supported by a National Institutes of Health grant to J.C.A.B and M.S.; J.C.A.B. is a PEW scholar. U.J. is a Burroughs Wellcome Fund Scholar.

Received: December 1, 2000

Revised: March 14, 2001

Accepted: March 15, 2001

#### References

1. Vijayalakshmi, J., Mukherjee, M.K., Graumann, J., Jakob, U., and Saper, M. (2001). The 2.2 Å crystal structure of Hsp33: a heat shock protein with redox-regulated chaperone activity. *Structure* 9, 367–375.
2. Jakob, U., Muse, W., Eser, M., and Bardwell, J.C.A. (1999). Chaperone activity with a redox switch. *Cell* 96, 341–352.
3. Aslund, F., and Beckwith, J. (1999). Bridge over troubled waters: sensing stress by disulfide bond formation. *Cell* 96, 751–753.
4. Ruddock, L.W., and Klappa, P. (1999). Oxidative stress: protein folding with a novel redox switch. *Curr. Biol.* 9, R400–402.
5. Jakob, U., Eser, M., and Bardwell, J.C.A. (2000). Hsp33's redox switch has a novel zinc-binding motif. *J. Biol. Chem.* 275, 38301–38310.
6. Barbirz, S., Jakob, U., and Glocker, M. (2000). Mass spectrometry unravels disulfide bond formation as the mechanism that activates a molecular chaperone. *J. Biol. Chem.* 275, 18759–18766.
7. Zheng, M., Aslund, F., and Storz, G. (1998). Activation of the OxyR transcription factor by reversible disulfide bond formation. *Science* 279, 1718–1721.
8. Kang, J.G., et al., and Roe, J.H. (1999). RsrA, an anti-sigma factor regulated by redox change. *EMBO J.* 18, 4292–4298.
9. Kuge, S., and Jones, N. (1994). YAP1 dependent activation of TRX2 is essential for the response of *Saccharomyces cerevisiae* to oxidative stress by hydroperoxides. *EMBO J.* 13, 655–664.
10. Kuge S., Jones, N., and Nomoto, A. (1997). Regulation of yAP-1 nuclear localization in response to oxidative stress. *EMBO J.* 16, 1710–1720.
11. Delaunay, A., Isnard, A.D., and Toledano, M.B. (2000). H(2)O(2) sensing through oxidation of the Yap1 transcription factor. *EMBO J.* 19, 5157–5166.
12. Knapp, L.T., and Klann, E. (2000). Superoxide-induced stimulation of protein kinase C via thiol modification and modulation of zinc content. *J. Biol. Chem.* 275, 24136–24145.
13. Buchner, J. (1996). Supervising the fold: functional principles of molecular chaperones. *FASEB J.* 10, 10–19.
14. Schmid, F.X. (1993). Spectral methods of characterizing protein conformation and conformational changes. In *Protein Structure: A Practical Approach*, T.E. Creighton, ed. (Oxford: Oxford University Press, pp. 251–284.
15. Creighton, T.E. (1992). In *Proteins: Structure and Molecular Properties*, T.E. Creighton, ed. (New York: W.H. Freeman and Company), p. 154.
16. Gutfreund, H. (1995). In *Kinetics for the Life Science: Receptors, Transmitters and Catalysts*, H. Gutfreund, ed. (Cambridge: Cambridge University Press), pp. 233–235.
17. Haslbeck, M., et al., and Buchner J. (1999). Hsp26: a temperature-regulated chaperone. *EMBO J.* 18, 6744–6751.
18. Zhang, R., and Snyder, G.H. (1989). Dependence of formation of small disulfide loops in two-cysteine peptides on the number and types of intervening amino acids. *J. Biol. Chem.* 31, 18472–18479.
19. Lee, G.J., Pokala, N., and Vierling, E. (1995). Structure and in vitro molecular chaperone activity of cytosolic small heat shock proteins from pea. *J. Biol. Chem.* 270, 10432–10438.
20. Zhu, X., et al., and Hendrickson, W.A. (1996). Structural analysis of substrate binding by the molecular chaperone DnaK. *Science* 272, 1606–1614.
21. Fenton, W.A., Kashi, Y., Furtak, K., and Horwich, A.L. (1994). Residues in chaperonin GroEL required for polypeptide binding and release. *Nature* 371, 614–619.
22. Sha, B., Lee, S., and Cyr, D.M. (2000). The crystal structure of the peptide binding fragment from the yeast Hsp40 protein Sis1. *Structure* 8, 799–807.
23. Gill, S.C., and von Hippel, P.H. (1989). Calculation of protein extinction coefficients from amino acid sequence data. *Anal. Biochem.* 182, 319–326.
24. Creighton, T.E. (1993). Disulfide bonds between cysteines. In *Protein Structure: A Practical Approach*, T.E. Creighton, ed. (Oxford: Oxford University Press), p. 155.

25. Wong, C., Sridhara, S., Bardwell, J.C.A., and Jakob, U. (2000). Heating greatly speeds Coomassie blue staining and destaining. *Biotechniques* 28, 426–432.
26. Hunt, J.B., Neece, S.H., and Ginsburg, A. (1985). The use of 4-(2-pyridylazo)resorcinol in studies of zinc release from *Escherichia coli* aspartate transcarbamoylase. *Anal. Biochem.* 146, 150–157.
27. Luther, M.A., Cai, G.Z., and Lee, L.C. (1986). Thermodynamics of dimer and tetramer formations in rabbit muscle phosphofructokinase. *Biochemistry* 25, 7931–7937.